J Arid Land (2023) 15(3): 344–358
https://doi.org/10.1007/s40333-023-0093-5

Science Press Springer-Verlag

Reclamation during oasification is conducive to the accumulation of the soil organic carbon pool in arid land

YANG Yuxin[1,2], GONG Lu[1,2,3*], TANG Junhu[1,2]

[1] College of Ecology and Environment, Xinjiang University, Urumqi 830017, China;
[2] Key Laboratory of Oasis Ecology, Ministry of Education, Urumqi 830017, China;
[3] Xinjiang Jinghe Observation and Research Station of Temperate Desert Ecosystem, Ministry of Education, Urumqi 830017, China

Abstract: Soil organic carbon (SOC) and its stable isotope composition reflect key information about the carbon cycle in ecosystems. Studies of carbon fractions in oasis continuous cotton-cropped fields can elucidate the SOC stability mechanism under the action of the human-land relationship during the oasification of arid land, which is critical for understanding the carbon dynamics of terrestrial ecosystems in arid lands under global climate change. In this study, we investigated the Alar Reclamation Area on the northern edge of the Tarim Basin, Xinjiang Uygur Autonomous Region of China, in 2020. In original desert and oasis farmlands with different reclamation years, including 6, 10, 18, and 30 a, and different soil depths (0–20, 20–40, 40–60 cm), we analyzed the variations in SOC, very liable carbon (C_{VL}), liable carbon (C_L), less liable carbon (C_{LL}), and non-liable carbon (C_{NL}) using the method of spatial series. The differences in the stable carbon isotope ratio ($\delta^{13}C$) and beta (β) values reflecting the organic carbon decomposition rate were also determined during oasification. Through redundancy analysis, we derived and discussed the relationships among SOC, carbon fractions, $\delta^{13}C$, and other soil physicochemical properties, such as the soil water content (SWC), bulk density (BD), pH, total salt (TS), total nitrogen (TN), available phosphorus (AP), and available potassium (AK). The results showed that there were significant differences in SOC and carbon fractions of oasis farmlands with different reclamation years, and the highest SOC was observed at the oasis farmland with 30-a reclamation year. C_{VL}, C_L, C_{LL}, and C_{NL} showed significant changes among oasis farmlands with different reclamation years, and C_{VL} had the largest variation range (0.40–4.92 g/kg) and accounted for the largest proportion in the organic carbon pool. The proportion of C_{NL} in the organic carbon pool of the topsoil (0–20 cm) gradually increased. $\delta^{13}C$ varied from –25.61‰ to –22.58‰, with the topsoil showing the most positive value at the oasis farmland with 10-a reclamation year; while the β value was the lowest at the oasis farmland with 6-a reclamation year and then increased significantly. Based on the redundancy analysis results, the soil physicochemical properties, such as TN, AP, AK, and pH, were significantly correlated with C_L, and TN and AP were positively correlated with C_{VL}. However, $\delta^{13}C$ was not significantly influenced by soil physicochemical properties. Our analysis advances the understanding of SOC dynamics during oasification, revealing the risk of soil carbon loss and its contribution to terrestrial carbon accumulation in arid lands, which could be useful for the sustainable development of regional carbon resources and ecological protection in arid ecosystem.

Keywords: oasification; soil organic carbon; carbon fractions; labile carbon; $\delta^{13}C$; arid land

Citation: YANG Yuxin, GONG Lu, TANG Junhu. 2023. Reclamation during oasification is conducive to the accumulation of the soil organic carbon pool in arid land. Journal of Arid Land, 15(3): 344–358. https://doi.org/10.1007/s40333-023-0093-5

*Corresponding author: GONG Lu (E-mail: gonglu721@163.com)
Received 2022-10-15; revised 2023-01-17; accepted 2023-01-28

1 Introduction

The soil carbon pool is an important part of the terrestrial carbon pool, with approximately 1550 Gt C stored in the form of organic carbon (Lal, 2004). As a natural sink of atmospheric CO_2, soil organic carbon (SOC) pool plays an important role in coordinating soils, vegetation, and their relationships with the surrounding environment (Wiesmeier et al., 2019; Bossio et al., 2020). The accumulation and turnover rates of SOC significantly influence the global carbon budget and the stability of the climate system, thus impacting the global carbon cycle and climate change (Carvalhais et al., 2014). Land use is considered to be the most important factor affecting the accumulation and decomposition of SOC, and in arid and semiarid regions, the oasification process involving the gradual transformation of original desert to oasis farmlands has become a typical manifestation of land conversion efforts in these regions (Malik et al., 2018; Xue et al., 2019). In this process, agricultural activities, such as different crop cover types, tillage measures, and exogenous material inputs, can alter the plant rhizosphere processes and affect the stability of SOC, in turn changing the soil carbon storage (Gui et al., 2011; Finzi et al., 2015; Gong et al., 2015). Therefore, obtaining a better understanding of SOC dynamics during oasification is essential for maintaining the stability of soil carbon pools in arid areas and the sustainable development of oasis farmlands.

However, SOC, due to its high background value, shows a certain hysteresis in response to changes in land use methods and cannot optimally reflect changes in the SOC content or conversion rate over short periods of time (Post and Kwon, 2000). SOC has been found to be a heterogeneous mixture of compounds with different turnover cycles, and its chemical structure affects its stability (Kan et al., 2022). In general, SOC pool can be chemically divided into very liable carbon (C_{VL}), liable carbon (C_L), less liable carbon (C_{LL}), and non-liable carbon (C_{NL}), among which C_{VL} and C_L are more sensitive to land use changes than soil total organic carbon (Chan et al., 2001; Nath et al., 2022). Several studies conducted in arid and semiarid regions have revealed that organic carbon fractions respond differently after land use changes, thus highlighting the unique sensitivity of these carbon fractions (Bremer et al., 1994; Yu et al., 2017; Zhong et al., 2019; He et al., 2021). For example, C_L and C_{NL} in surface soils converted from original desert to croplands in the Yanqi Basin of Xinjiang Uygur Autonomous Region, China, increased significantly (Zhang et al., 2014). However, little research has been conducted on oasification in arid and semiarid regions, and research on carbon fractions after the conversion of original desert into oasis farmlands with different reclamation years is especially scarce. The stability and dynamic changes that occur in soil carbon pool during the oasification process in arid regions are still unclear.

Carbon stable isotope techniques can be used to describe the distribution of organic carbon, analyze the dynamics of SOC by studying the variation in stable carbon isotope ratio ($\delta^{13}C$), and interpret the turnover characteristics of organic carbon (Nissenbaum and Schallinger, 1974; Schaub and Alewell, 2009; Wang et al., 2018). In studies of $\delta^{13}C$, the slope of the linear regression between the logarithm of SOC content and $\delta^{13}C$ is defined as beta (β) value; this term can be used as a representative of the organic carbon decomposition rate. The smaller the β value is, the faster the decomposition rate of SOC is (Zhao et al., 2019; Liu et al., 2021). During land use changes in arid or semiarid land areas, SOC content and distribution as well as $\delta^{13}C$ values vary with the degree of human disturbance (Liu et al., 2010; Sharafatmandrad, 2019; Zhu et al., 2021). Therefore, it is important to investigate the trends and patterns of SOC and its fractions during the process of oasification to improve the soil carbon storage capacity, understand the stability of the soil carbon pool, and maintain the healthy development of oasis ecosystems.

The oasis-desert ecotone at the northern edge of the Tarim Basin is the most representative oasis agricultural area and the main storage area of SOC in arid land. To support regional economic development, the exploitation of soil and water resources in this region has been expanding. The original desert has been gradually transformed into oasis farmlands through agricultural activities (e.g., tillage, irrigation, and fertilization), making the region an important area of continuous cotton cropping in China. Moreover, the stock of SOC has also changed in response to the conversion of

original desert to oasis farmlands (Zhang et al., 2003; Bai et al., 2021; Xue et al., 2022). Therefore, a deeper study of the stability of SOC pool during oasification is particularly important.

To address this gap in knowledge, we selected original desert and oasis farmlands with different reclamation years to determine SOC and its fractions, $\delta^{13}C$, and other soil physicochemical properties. The objectives of this study were to probe the changes in SOC and the distribution patterns of its fractions during oasification, investigate the changes in the $\delta^{13}C$ and β values that occur during oasification, and elucidate the effects of other physicochemical factors on SOC, carbon fractions, $\delta^{13}C$, and β values. Through this study, we aim to understand the ecological processes of soil carbon cycling during oasification in arid land to promote the sustainable development of regional carbon resources and provide a scientific basis for the study of the "carbon source and sink" effect in oases.

2 Materials and methods

2.1 Study area

The Alar Reclamation Area is located at the northern edge of the Tarim Basin and the southern foot of the middle Tianshan Mountains, Xinjiang Uygur Autonomous Region of China. This region belongs to the alluvial plain area of the Tarim River, with slightly elevated terrain along the riverbanks and on both sides of the alluvial ditch; the terrain is also inclined from northwest to southeast. This area spans 281 km from east to west and 180 km from north to south, with an average elevation of 1012 m. Rainfall is scarce. Little snow falls in winter, and evaporation is strong on the land surface. The average annual precipitation ranges from 40.1 to 82.5 mm, and the average annual evaporation ranges from 1876.6 to 2558.9 mm. This area has good light and heat conditions and great temperature differences between day and night (Zhang, 2016). The local soil is alkaline and contains a high amount of salt (Peng et al, 2019). The main variety of planted cotton is "Xinluzhong 82", which is managed with the local integrated farming management methods, in which drip irrigation is applied 5–7 times during the reproductive period; the basal fertilizer applied comprises diammonium phosphate, urea, potassium sulfate, and mixed organic fertilizer.

2.2 Sample collection

Field soil samples were collected during June–July in 2020. In general, the closer the land area was to the inflow river, the earlier the oasis was formed. Therefore, old oases reclaimed as early as the 1950s and new oases reclaimed in recent years are distributed along the river to the inland region within the desert-oasis ecotone of the Alar Reclamation Area (Huang et al., 2021). We applied the spatial series method instead of the temporal series method to select four cotton fields with different reclamation years (i.e., 6, 10, 18, and 30 a) in a region with a similar geographical location and soil texture; irrigation was withheld from these fields for 15 d before sampling. The control group (CK) was an original desert with vegetation coverage consisting mainly of *Alhagi sparsifolia*, *Tamarix* spp., and *Karelinia caspica* (Ling et al., 2014). Each sample plot was approximately 0.12 hm^2. After cotton harvest in October 2019, three typical sample squares with 1 m×1 m areas were selected in each of the above sites with different reclamation years to collect soil samples by the quarter method. After removing obvious root residues, stones, and other debris, we crushed the soil samples and mixed them thoroughly before bringing them back to the laboratory for natural air-drying, grinding, and sieving to determine SOC content, carbon fractions, and other basic soil physicochemical properties.

2.3 Laboratory analysis

The content of SOC and its fractions was tested by the potassium dichromate method. According to the principle of the Walkley and Black method, the reaction heat produced by different concentrations of concentrated sulfuric acid resulted in different degrees of SOC oxidation (Walkley and Black, 1934; Chan et al., 2001). The carbon fraction oxidized by 6 mol/L sulfuric acid was regarded as C_{VL}. The difference in oxidizible organic carbon extracted between 9 and 6 mol/L sulfuric acid were regarded as C_L. The difference in oxidizible organic carbon extracted

between 9 and 12 mol/L sulfuric acid were regarded as C_{LL}. The carbon fraction oxidized by 12 mol/L H_2SO_4 when compared with the total organic carbon was regarded as C_{NL}.

Soil water content (SWC) was measured by the drying method. The soil samples were dried to a constant weight at 105°C, and the wet and dry weights of the soil samples were recorded. We used the cutting ring method to determine bulk density (BD). The original-state soil samples taken by the cutting ring were brought back to the laboratory and dried to a constant weight at 105°C. After cooling, the dry weights were measured, and BD were calculated (Huntington et al., 1989). A total of 20-g soil was dried and passed through a 1-mm sieve, and 100-mL distilled water was added for shock filtration. Soil pH was determined by using a pH meter (PHS-3C, Shanghai Yidian Scientific Instrument Co. Ltd., Shanghai, China). Total salt (TS) content was the sum of the eight ions' concentrations (including CO_3^{2-}, HCO_3^-, Cl^-, SO_4^{2-}, Ca^{2+}, Mg^{2+}, Na^+, and K^+). CO_3^{2-} and HCO_3^- were determined by the double indicator neutral method; Cl^- was determined by the $AgNO_3$ (Mohrs's titration) method; SO_4^{2-} was determined by indirect Ethylene Diamine Tetraacetic Acid (EDTA) titration; Ca^{2+} and Mg^{2+} were determined by complexometric titration with EDTA; and Na^+ and K^+ were determined by flame photometry. Total nitrogen (TN) was determined by the Kjeldahl method (K370, BUCHI Labortechnik AG, Flawil, Switzerland). Available phosphorus (AP) was extracted with $NaHCO_3$ and determined by colorimetry. Available potassium (AK) was determined by the flame photometry method.

The expression of $\delta^{13}C$ is as follows (Breecker et al., 2015):

$$\delta^{13}C=\left[\frac{\left({}^{13}C/{}^{12}C\right)_{\text{sample}}}{\left({}^{13}C/{}^{12}C\right)_{\text{standard}}}-1\right]\times 1000‰\,, \tag{1}$$

where $\delta^{13}C$ is stable carbon isotope ratio (‰), which is used to describe the variation in the ^{13}C when a sample is compared to a standard sample (the error of $\delta^{13}C$ is ±0.2‰); $(^{13}C/^{12}C)_{sample}$ is the ratio of ^{13}C to ^{12}C in the sample; and $(^{13}C/^{12}C)_{standard}$ is the ratio of ^{13}C to ^{12}C in standard material of Pee Dee Belemnite (PDB) in South Carolina, USA, which is defined as $^{13}C/^{12}C$=0.01124 (O'Leary, 1981).

2.4 Statistical analysis

The data obtained in this study were first organized and analyzed in Excel 2016 for the basic statistical analysis; then, analysis of variance and least significant difference were used to test SOC, carbon fractions, $\delta^{13}C$, and other physicochemical factors in different reclamation years and soil depths and to analyze the interaction between the soil depth and reclamation years using SPSS 22.0 software. The Kruskal-Wallis test was used to compare the variability in β values among different reclamation years. Canoco 5.0 software was selected for the redundancy analysis (RDA) to investigate the correlations among carbon fractions, $\delta^{13}C$, and other physicochemical factors of the soil. Pearson correlation analysis was used to analyze the correlations among SOC, $\delta^{13}C$, and soil environmental factors. Origin 2020 and R Studio were used for plotting.

3 Results

3.1 Variations of soil physicochemical properties during oasification

The physicochemical properties of the soil samples are presented in Table 1. SWC measured at different soil depths remained the lowest in original desert (CK), with BD ranging from 1.25 to 1.43 g/cm^3. The value of pH was the highest in original desert (8.66). The soil was alkaline, with a decreasing trend observed alongside continuous tillage. Variations in TS was large, ranging from 1.59 to 18.31 g/kg. TN, AP, and AK contents tended to be highest at the soil depth of 0–20 cm after 6-a reclamation. The effects of reclamation year, soil depth, and their interaction on soil physicochemical properties are shown in Table 2. Soil physicochemical properties except AK were significantly affected by reclamation year. Soil depth had significant effects on SWC, BD, TS, TN, and AP. Among them, BD, TN, and AP were significantly affected by the interaction between reclamation year and soil depth (P<0.05).

Table 1 Variations of physicochemical properties in different reclamation years and soil depths

Reclamation year	Soil depth (cm)	SWC (%)	BD (g/cm^3)	pH	TS (g/kg)	TN (g/kg)	AP (mg/kg)	AK (mg/kg)
CK	0–20	10.62±1.50	1.37±0.04	8.66±0.14	18.31±14.26	0.25±0.03	2.99±0.35	164.53±19.42
	20–40	12.18±1.60	1.36±0.05	8.39±0.14	9.98±1.65	0.20±0.04	3.73±0.95	170.22±18.46
	40–60	13.69±1.73	1.43±0.05	8.31±0.04	6.28±0.73	0.24±0.03	3.59±0.50	162.49±22.87
6-a	0–20	18.68±1.32	1.29±0.04	8.07±0.05	6.53±3.54	0.37±0.03	18.33±5.89	185.81±31.15
	20–40	24.96±1.79	1.27±0.03	8.04±0.03	2.23±1.26	0.32±0.03	19.85±4.94	177.88±16.29
	40–60	26.25±1.41	1.40±0.04	8.15±0.11	1.59±0.50	0.26±0.03	11.15±2.09	171.90±21.23
10-a	0–20	21.29±1.57	1.25±0.02	7.96±0.12	7.41±4.68	0.56±0.03	28.27±3.99	229.31±49.75
	20–40	26.09±1.49	1.27±0.03	7.98±0.03	2.51±0.71	0.46±0.07	21.20±4.45	201.76±96.14
	40–60	28.69±2.61	1.28±0.04	8.01±0.07	1.98±0.80	0.37±0.09	17.84±3.95	211.91±65.23
18-a	0–20	20.88±0.99	1.28±0.02	7.92±0.21	14.01±5.37	0.55±0.06	30.53±5.09	213.26±23.62
	20–40	25.49±1.53	1.27±0.05	7.82±0.23	6.76±2.77	0.54±0.04	22.80±5.41	227.52±27.83
	40–60	28.59±2.35	1.26±0.02	7.81±0.19	2.14±0.22	0.41±0.05	14.85±2.11	211.34±17.06
30-a	0–20	21.80±1.56	1.32±0.04	7.80±0.13	16.29±5.33	0.58±0.05	31.30±1.66	211.08±42.75
	20–40	24.62±1.15	1.33±0.02	7.81±0.04	8.35±3.85	0.47±0.09	21.54±4.17	208.82±31.43
	40–60	24.72±1.69	1.36±0.02	7.82±0.17	4.24±0.53	0.33±0.04	15.51±2.80	205.05±20.43

Note: CK, original desert; SWC, soil water content; BD, bulk density; TS, total salt; TN, total nitrogen; AP, available phosphorus; AK, available potassium. Mean±SD.

Table 2 Effects of reclamation year, soil depth, and their interaction on soil physicochemical properties

Source	Controlled variable	Sum of square	*df*	Mean square	*F* value	*P* value
SWC	Reclamation year	1093.22	4	273.31	98.32	<0.01
	Soil depth	259.77	2	129.88	46.72	<0.01
	Reclamation year×Soil depth	44.19	8	5.52	1.99	0.08
BD	Reclamation year	0.07	4	0.02	14.35	<0.01
	Soil depth	0.01	2	0.01	4.68	0.02
	Reclamation year×Soil depth	0.02	8	0.01	2.56	0.03
pH	Reclamation year	2.40	4	0.60	35.73	<0.01
	Soil depth	0.05	2	0.02	1.37	0.27
	Reclamation year×Soil depth	0.20	8	0.03	1.51	0.19
TS	Reclamation year	443.60	4	110.90	5.13	0.03
	Soil depth	679.98	2	339.99	15.74	<0.01
	Reclamation year×Soil depth	84.58	8	10.57	0.49	0.85
TN	Reclamation year	0.49	4	0.12	49.93	<0.01
	Soil depth	0.14	2	0.07	29.75	<0.01
	Reclamation year×Soil depth	0.06	8	0.01	3.18	0.01
AP	Reclamation year	2506.30	4	626.58	46.14	<0.01
	Soil depth	705.92	2	352.96	25.99	<0.01
	Reclamation year×Soil depth	343.52	8	42.94	3.16	0.01
AK	Reclamation year	19450.03	4	4862.51	3.07	0.31
	Soil depth	514.99	2	257.50	0.16	0.85
	Reclamation year×Soil depth	1563.37	8	195.42	0.12	0.99

Note: *df* is degree of freedom.

3.2 Variations of soil organic carbon (SOC) and carbon fractions during oasification

SOC varied significantly during the process of oasification (Table 3). At different soil depths,

SOC was the highest at the oasis farmland with 10-a reclamation year. C_{VL} had a wide range of variation (0.40–4.92 g/kg) and showed the highest accumulation at the soil depth of 20–40 cm at the oasis farmland with 30-a reclamation year. The highest C_{NL} (3.62 g/kg) was also observed at the oasis farmland with 30-a reclamation year, and the lowest was observed in original desert (CK). C_{VL} changed significantly among different reclamation years and soil depths, while C_L, C_{LL}, and C_{NL} exhibited significant changes only among different reclamation years (Table 4). SOC was significantly correlated with C_{VL} (R^2=0.94; P<0.01), C_L (R^2=0.42; P<0.01), C_{LL} (R^2=0.38; P<0.01), and C_{NL} (R^2=0.88; P<0.01) in all reclamation years and soil depths (Fig. 1). At the soil depths of 0–20 and 20–40 cm, SOC pool were dominated by liable fractions (i.e., C_{VL}, C_L, and C_{LL}) (Fig. 2). At the soil depth of 0–20 cm, C_{NL} (18.63%–34.52%) showed a gradual increase with increasing reclamation years. At the soil depth of 40–60 cm, C_{NL} accounted for the main proportion (56.30%) of each carbon fraction in original desert.

Table 3 Variations of soil organic carbon (SOC) and carbon fractions in different reclamation years and soil depths

Reclamation year	Soil depth (cm)	C_{VL} (g/kg)	C_L (g/kg)	C_{LL} (g/kg)	C_{NL} (g/kg)	SOC (g/kg)
CK	0–20	0.66±0.12	0.21±0.05	0.40±0.08	0.29±0.07	1.44±0.21
	20–40	0.53±0.17	0.19±0.01	0.24±0.14	0.36±0.18	0.93±0.24
	40–60	0.40±0.08	0.08±0.01	0.12±0.03	0.77±0.33	1.20±0.32
6-a	0–20	1.56±0.06	0.72±0.30	0.08±0.02	0.60±0.28	2.99±0.20
	20–40	1.04±0.14	0.28±0.08	0.04±0.01	0.64±0.01	1.88±0.38
	40–60	0.61±0.05	0.16±0.08	0.05±0.02	0.48±0.07	1.30±0.18
10-a	0–20	2.13±0.39	0.56±0.36	0.45±0.20	0.72±0.28	3.86±0.83
	20–40	1.46±0.60	0.74±0.44	0.19±0.09	0.51±0.18	2.90±1.12
	40–60	0.82±0.05	0.64±0.24	0.32±0.18	0.29±0.07	2.07±0.08
18-a	0–20	1.80±0.28	0.84±0.28	0.13±0.05	0.96±0.14	3.67±0.21
	20–40	1.24±1.07	1.44±0.90	0.29±0.18	0.66±0.28	3.24±1.02
	40–60	0.74±0.70	0.59±0.33	0.37±0.14	0.37±0.12	2.07±1.75
30-a	0–20	4.34±0.47	1.97±0.41	0.56±0.08	3.62±0.59	10.48±0.59
	20–40	4.92±0.64	0.98±0.51	0.64±0.14	3.08±0.53	9.63±0.53
	40–60	0.60±1.12	1.49±0.48	0.64±0.14	2.15±1.19	7.74±2.15

Note: C_{VL}, very liable carbon; C_L, liable carbon; C_{LL}, less liable carbon; C_{NL}, non-liable carbon. Mean±SD.

Table 4 Effects of reclamation year, soil depth, and their interaction on carbon fractions

Source	Controlled variable	Sum of square	*df*	Mean square	*F* value	*P* value
C_{VL}	Reclamation year	76.03	4	19.01	79.73	<0.01
	Soil depth	6.27	2	3.13	13.14	<0.01
	Reclamation year×Soil depth	2.64	8	0.33	1.38	0.24
C_L	Reclamation year	9.57	4	2.39	21.07	<0.01
	Soil depth	0.54	2	0.27	2.38	0.11
	Reclamation year×Soil depth	2.66	8	0.33	2.93	0.02
C_{LL}	Reclamation year	1.44	4	0.36	8.50	<0.01
	Soil depth	0.02	2	0.01	0.18	0.84
	Reclamation year×Soil depth	0.31	8	0.04	0.93	0.51
C_{NL}	Reclamation year	41.56	4	10.39	47.35	<0.01
	Soil depth	1.35	2	0.68	3.08	0.06
	Reclamation year×Soil depth	3.18	8	0.40	1.81	0.12
SOC	Reclamation year	370.84	4	92.71	118.04	<0.01
	Soil depth	19.44	2	9.72	12.38	<0.01
	Reclamation year×Soil depth	6.03	8	0.75	0.96	0.48

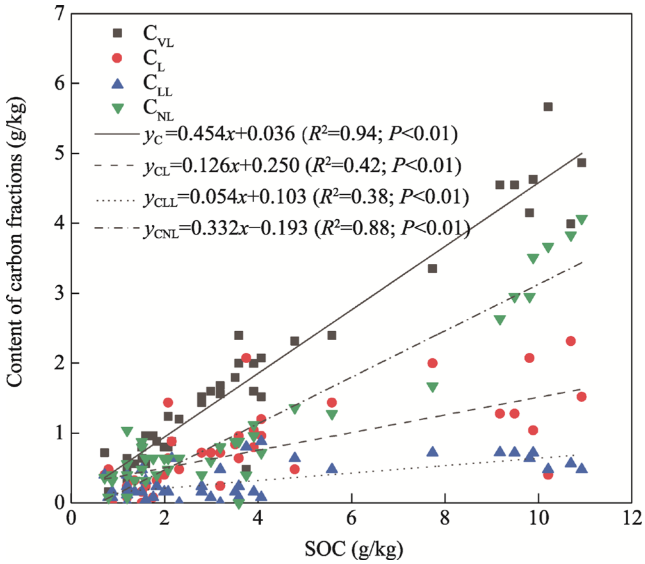

Fig. 1 Relationships of soil organic carbon (SOC) with different carbon fractions. C_{VL}, very liable carbon; C_L, liable carbon; C_{LL}, less liable carbon; C_{NL}, non-liable carbon.

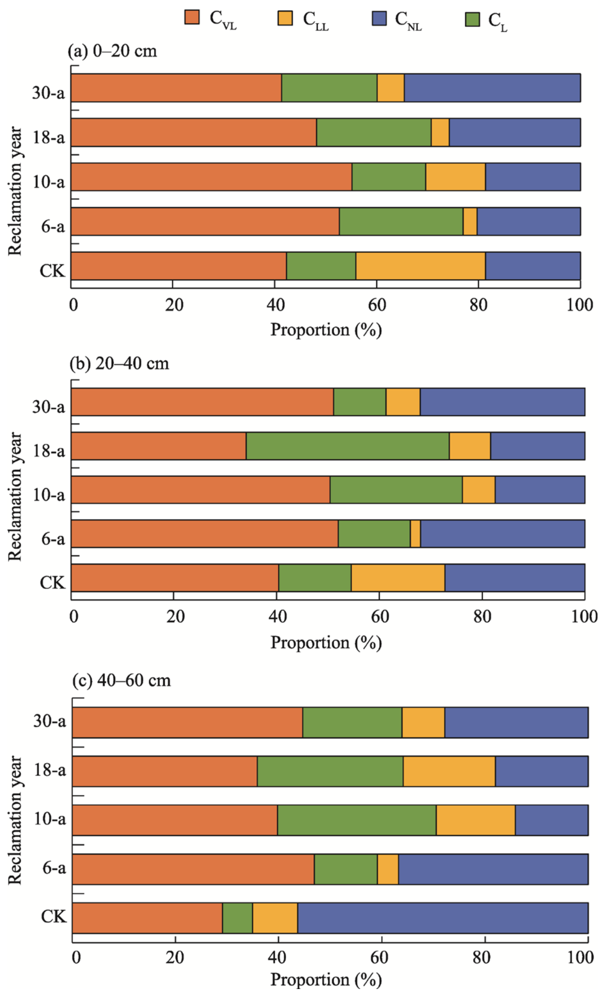

Fig. 2 Proportions of C_{VL}, C_L, C_{LL}, and C_{NL} in total SOC at the soil depth of 0–20 cm (a), 20–40 cm (b), and 40–60 cm (c). CK, original desert.

3.3 Variations of stable carbon isotope ratio ($\delta^{13}C$) and beta (β) value during oasification

As shown in Figure 3, $\delta^{13}C$ varied significantly (from –25.61‰ to –22.58‰) with reclamation years and soil depths. $\delta^{13}C$ value at the soil depths of 0–20 and 40–60 cm changed significantly (P<0.05) among different reclamation years. Among them, at the soil depth of 0–20 cm, $\delta^{13}C$ showed a significant increase at the oasis farmland with 10-a reclamation year. At the soil depth of 20–40 cm, the variation in $\delta^{13}C$ in each reclamation period fluctuated but was not significant. At the soil depth of 40–60 cm, $\delta^{13}C$ showed significant decreases at the oasis farmlands with 6-a and 10-a reclamation year and significant increases at the oasis farmlands with 18-a and 30-a reclamation year (P<0.05). $\delta^{13}C$ changed significantly among different soil depths at the oasis farmland with 10-a reclamation year (P<0.05). In addition, β values ranged throughout the process of oasification in oasis farmlands with the following rank: 18-a>10-a>30-a>CK>6-a. In addition, there was a significant increase from the oasis farmlands with 6-a reclamation year to the oasis farmlands with 10-a reclamation year (Fig. 4).

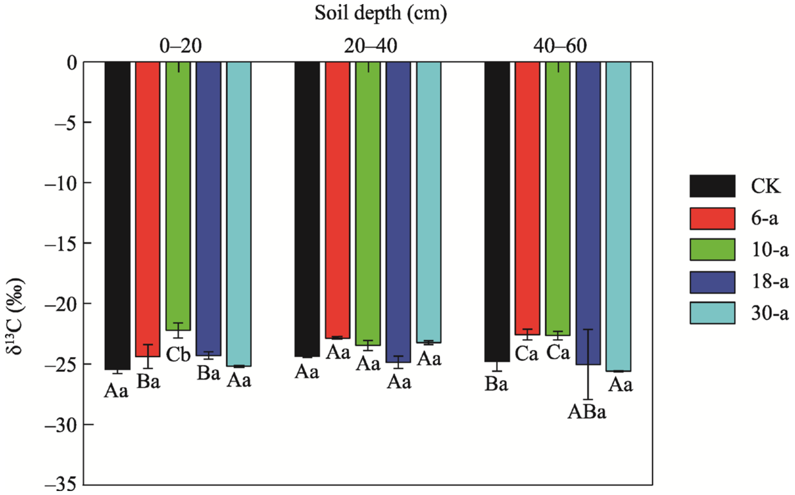

Fig. 3 Changes of stable carbon isotope ratio ($\delta^{13}C$) in different reclamation years and at different soil depths. Different lowercase letters represent the significant differences among the three soil depth in the same reclamation year (P<0.05), and different uppercase letters represent the significant difference among different reclamation years at the same soil depth (P<0.05). Bars mean standard errors.

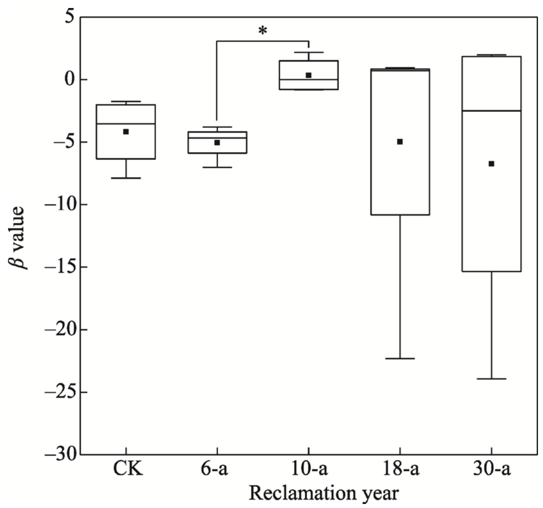

Fig. 4 Changes of beta (β) value in different reclamation years. * denotes significant at P<0.05 level based on the Kruskal-Wallis (KW) test. The top, middle, and bottom lines of the box represent the upper quartile, median, and lower quartile, respectively; the black dot in the box represents the mean; and the top bar and bottom bar represent the maximum and minimum, respectively.

3.4 Effect of soil physicochemical properties during ossification

The ordination relationships among SOC, carbon fractions, $\delta^{13}C$, and other soil physicochemical properties are shown in Figure 5. Among them, TN, pH, AP, and AK exhibited the longest connecting lines, and the cosine value of the angle between C_{VL} and C_L was relatively large. These results suggested that TN, pH, AP, and AK have large correlation coefficients with carbon fractions and are positively correlated, except for pH. TN, AP, AK, and pH greatly influenced on the transformation of SOC. The connecting lines of SWC and TS were long, but the cosine value of this angle was relatively low. SWC and TS were positively correlated with carbon fractions, but these correlations were not obvious. Low cosine values were observed between $\delta^{13}C$ and soil physicochemical properties, though these correlations were not significant. The effects of seven soil physicochemical properties on carbon fractions differed. The results showed that the order of importance was TN>pH>AP>AK>TS>SWC>BD (Table 5). Among them, the effects of TN, AP, pH, and AK on carbon fractions reached significant levels (P<0.05), while the effects of TS, SWC, and BD on SOC, carbon fractions, and $\delta^{13}C$ did not reach the significant level (P>0.05; Table 6).

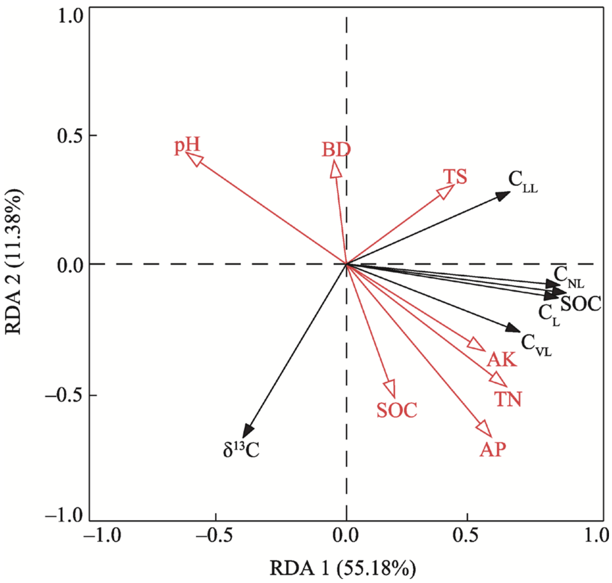

Fig. 5 Redundancy analysis (RDA) of SOC, carbon fractions, and $\delta^{13}C$ with soil physicochemical properties. SWC, soil water content; BD, bulk density; TS, total salt; TN, total nitrogen; AP, available phosphorus; AK, available potassium.

Table 5 Importance and significance level of soil environmental factors to SOC, carbon fractions, and $\delta^{13}C$

Soil environmental factor	Rank	Proportion (%)	*F* value	*P* value
TN	1	26.1	4.6	0.016
pH	2	25.5	4.5	0.024
AP	3	24.3	4.2	0.020
AK	4	20.4	3.3	0.036
TS	5	12.1	1.8	0.162
SWC	6	6.4	0.9	0.432
BD	7	3.7	0.5	0.666

4 Discussion

4.1 Effect of oasification on SOC

In this study, different reclamation years were found to significantly affect SOC, and a significant

Table 6 Correlation analysis of SOC, carbon fractions, and δ^{13}C with soil physicochemical properties

	SWC	BD	pH	TS	TN	AP	AK
SOC	0.86	–0.51	–0.76	0.29	0.96	0.93	0.45
C_{VL}	0.16	–0.19	–0.49	0.38	0.66**	0.63*	0.44
C_L	0.37	–0.28	–0.72**	0.23	0.70**	0.66**	0.68**
C_{LL}	0.11	0.00	–0.36	0.30	0.35	0.22	0.48
C_{NL}	0.13	0.14	–0.51	0.35	0.44	0.45	0.31
δ^{13}C	0.38	–0.29	–0.09	–0.47	0.09	0.25	0.12

Note: * and ** denote significant at $P<0.05$ and $P<0.01$ levels, respectively.

increase in SOC was observed in the whole soil profile after reclamation from the original desert to continuously cropped farmlands (Table 3). This finding is consistent with the conclusions of previous research that the carbon sequestration process that occurs in arable lands under agricultural tillage is of a greater magnitude than that which occurs in uncultivated soils (DeGryze et al., 2004). The reason for this difference may be that crop residues are effectively accumulated in soils during the reclamation and cultivation of oasis farmlands (Rakkar and Blanco-Canqui, 2018). At the same time, the large amount of organic fertilizer applied impacts the physical and chemical processes of the soil and accelerates biological processes within the soil, thereby accelerating the biodegradation of organic carbon (Vázquez et al., 2016; Zhou et al., 2022). Crops absorb water and nutrients from the soil through their root systems while growing and developing, so the humus layer of soil in oasis farmlands is thicker than that in the original desert (Jobbágy and Jackson, 2000; Nakamoto et al., 2012; Zhang et al., 2014). The increased root biomass promotes the formation and stability of soil aggregates, and the increased stability of the soil structure contributes to the accumulation of SOC (Li et al., 2020; Okolo et al., 2020).

In this study, SOC and C_{VL} were found to be highly and significantly influenced by soil depth. With the increase of soil depth, SOC and C_L decreased (Table 3). When a large amount of litter accumulates and is converted into organic matter on the soil surface, the carbon source supplementation obtained in deeper soil layers is reduced, and the microbial activity is also reduced, thus affecting the contents of more active carbon fractions, such as C_{VL}, C_L, and C_{LL}; this process is consistent with the findings of many other studies performed in arid areas (Cotrufo et al., 2015; Joly et al., 2020). The proportions of these more active carbon fractions in the total organic carbon reflect the quality and stability of SOC to a certain extent. In the results, the proportions of carbon fractions, except C_{NL}, in the topsoil decreased during the process of oasification (Fig. 2), indicating that the deepening of reclamation could promote the conversion of active organic carbon to passive organic carbon and thereby improve the stability of carbon pool.

In the SOC pool of oasis farmlands, SOC was significantly correlated with C_{VL}, C_L, and C_{LL} (Fig. 1). The proportion of C_{NL} at the soil depth of 0–40 cm was lower than the proportion of the sum of the active carbon fractions (C_{VL}, C_L, and C_{LL}) (Fig. 2). This finding was not consistent with the results of previous studies (Rovira et al., 2012; Zhang et al., 2014; Ahmed et al., 2016). Original desert in arid lands has low initial SOC. When original desert is reclaimed into oasis farmlands, the input of organic matter provides a sufficient carbon source for microbial growth and reproduction and accelerates the decomposition of organic matter in soil surface (Prommer et al., 2019). Because the sources of soil active organic carbon are microorganisms, which are active in crop residues, the increased microbial metabolic functions and secretions are important reasons for the increased carbon fractions being more easily decomposed during the conversion of original desert into oasis farmlands (Rovira and Vallejo, 2002). Compared to carbon, which is difficult to decompose, active organic carbon has a higher turnover rate and is more sensitive to soil physicochemical properties (e.g., pH and SWC), suggesting that the oasification process by which original desert is conversion to oasis farmlands increases SOC but also risks carbon loss (Benbi et al., 2015; Guan et al., 2022). It is noteworthy that in surface soils, although C_{NL} accounts for a relatively low proportion of the total SOC (Fig. 2), this fraction has a gradually

increasing trend, revealing the promotional effect of the oasification process on the terrestrial carbon storage capacity in arid lands.

4.2 Effect of oasification on soil $\delta^{13}C$ and β value

The organic carbon isotope composition is extremely weakly fractionated during the decomposition of plant residues and the layer-by-layer accumulation process (Wang et al., 2017; Li et al., 2022). The isotope values obtained in this study ranged from –25.61‰ to –22.58‰ (Fig. 3), slightly higher than the average isotope value of C_3 plants; our result was similar to the findings of other studies (de Rouw et al., 2015; Chen et al., 2018), indicating that $\delta^{13}C$ becomes enriched in the studied soils. The reason for this may be the fractionation of organic carbon isotopes. Compared to ^{13}C, ^{12}C more easily enters the CO_2 produced by the decomposition of soil organic matter, and ^{13}C increases $\delta^{13}C$ value in the soil by forming SOC (Li and Schaeffer, 2020). At different soil depths, $\delta^{13}C$ values at the oasis farmlands with 6-a and 10-a reclamation year were significantly positive compared to other oasis farmlands (Fig. 3); this finding may have been related to the improvements in microbial activity and fecundity caused by soil environmental changes that occur during the tillage process, as these improvements are conducive to the degradation of refractory substances in crops (Wynn et al., 2006; Brunn et al., 2014; Xiao et al., 2019; Sokol et al., 2022). However, $\delta^{13}C$ showed a significant negative tendency at the oasis farmlands with 18-a and 30-a reclamation year (Fig. 3), indicating that the degradation of microorganisms has a certain limit. The reason for this may be that agricultural activities such as tillage and irrigation can accelerate infiltration and precipitation (Blaser and Conrad, 2016). With the input of crop litter to soil surface during the tillage process, lignin, cellulose, and other refractory substances accumulate in the soil, resulting in a decrease in $\delta^{13}C$ (Gao et al., 2016). Meanwhile, β value can indicate the decomposition rate of SOC (Zhang et al., 2021). In the results, β value at the oasis farmland with 6-a reclamation year was the lowest and changed significantly compared with that at the oasis farmland with 10-a reclamation year (Fig. 4), indicating that the main reason for the positive $\delta^{13}C$ values measured at the oasis farmland with 6-a reclamation year was the increase in the decomposition rate. However, the decomposition rate of the samples at the oasis farmland with 10-a reclamation year was low but was still positive, which may have been related to the high SWC at the oasis farmland with 10-a reclamation year accelerating the migration and accumulation of organic carbon in the soil.

4.3 Interaction between soil carbon and soil physicochemical properties

Microorganisms secrete extracellular enzymes that participate in the metabolic processes of soil organic matter, thus procuring energy for themselves. When the demand for carbon sources increases, the related enzyme activities increase (Trivedi et al., 2016; Calabrese et al., 2022). In this study, C_{VL} and C_L had significant correlations with TN (Fig. 5); this may have been related to the application of fertilizers during tillage. On the one hand, nitrogen in soil contributes to condensation with lignin and other substances in crop residues, inhibits the activity of enzymes in decomposing passive organic carbon, and forms heterocyclic substances (such as indole) and phenols, which are difficult to decompose, thus promoting the accumulation of soil passive organic carbon (Ma et al., 2022). On the other hand, nitrogen can increase the production of organic matter such as lignin and other materials that are difficult to degrade, which may cause elevated soil passive organic carbon contents and distribution ratios, thus improving the stability of the soil carbon pool (Chen et al., 2018). AP and AK in soil samples showed significant increases throughout the process of oasification and were highly significantly correlated with C_{VL} or C_L (Fig. 5; Table 5), indicating that an increase in phosphorus in soil may have a stimulating effect leading to the mineralization of organic carbon. Therefore, the nutritional status of oasis farmlands can be improved, and this improvement is conducive to the absorption and utilization of soil nutrients by crop roots (Nottingham et al., 2015; Tan et al., 2017; Woittiez et al., 2019; Lu et al., 2020).

In arid areas, the salt in groundwater tends to move upward to the crop rhizosphere with the

evaporation of soil water and easily accumulates in the soil surface, resulting in alkaline soils (Zhang et al., 2014). The soil pH affects the mineralization and decomposition of SOC mainly by influencing microbial and enzyme activities and therefore has an inhibitory effect at high pH values (pH>8.5), decelerating the turnover of SOC (Malik et al., 2018). With the reclamation of oasis farmlands, a significant decrease in the soil pH (from 8.66 to 7.80) and a significant negative correlation between the soil pH and C_L can be observed (Tables 1, 2, and 6; Fig. 5), suggesting that a decline in soil alkalinity contributes to increases in microbial activities and the reproduction rate, which in turn benefit mineral adsorption by microbial residues and improve the decomposition of organic matter, resulting in the increased proportion of the active carbon pool throughout the oasification process.

5 Conclusions

SOC and its stable isotope composition were studied by the method of spatial series instead of temporal series in soil samples with different reclamation years in Alar Reclamation Area, Xinjiang Uygur Autonomous Region of China. The effects of soil physicochemical properties were analyzed to better understand the soil carbon dynamics during oasification process. The results showed that SOC and carbon fractions of oasis farmlands varied significantly among the regions with different reclamation years, and the highest SOC was observed at the oasis farmland with 30-a reclamation year. With the increase of soil depth, SOC reduced. C_{VL} had the largest variation range (0.40–4.92 g/kg) and accounted for the largest proportion in the SOC pool. The proportion of carbon fractions except C_{NL} decreased during oasification, but still occupied the main component. However, the proportion of C_{NL} in the carbon pool of topsoil (0–20 cm) gradually increased. $\delta^{13}C$ varied from –25.61‰ to –22.58‰, with the topsoil showing the most positive value at the oasis farmland with 10-a reclamation year; the β value was the lowest at the oasis farmland with 6-a reclamation year and then increased significantly. The redundancy analysis results showed that TN and AP were positively correlated with C_{VL}. The main soil physicochemical properties influencing C_L were TN, AP, AK, and pH. Oasification process, the conversion from original desert to oasis farmlands, altered the physicochemical properties of natural arid land soil, contributing to the storage of organic carbon in the arid ecosystem in northwestern China. These results provide a scientific basis for the study of the "carbon source and sink" effect in oases.

Acknowledgements

This study was supported by the Scientific Research Program of the Higher Education Institution of Xinjiang (XJEDU2021I1005). The authors express appreciation for the editors and anonymous reviewers, who helped improve the quality of this manuscript, and also express their gratitude to the farmers involved in this study during the field sampling.

References

Ahmed I U, Smith A R, Jones D L, et al. 2016. Tree species identity influences the vertical distribution of labile and recalcitrant carbon in a temperate deciduous forest soil. Forest Ecology and Management, 359: 352–360.

Bai J, Li J L, Bao A M, et al. 2021. Spatial-temporal variations of ecological vulnerability in the Tarim River Basin, Northwest China. Journal of Arid Land, 13(8): 814–834.

Benbi D K, Brar K, Toor A S, et al. 2015. Total and labile pools of soil organic carbon in cultivated and undisturbed soils in northern India. Geoderma, 237–238: 149–158.

Blaser M, Conrad R. 2016. Stable carbon isotope fractionation as tracer of carbon cycling in anoxic soil ecosystems. Current Opinion in Biotechnology, 41: 122–129.

Bossio D A, Cook-Patton S C, Ellis P W, et al. 2020. The role of soil carbon in natural climate solutions. Nature Sustainability, 3(5): 391–398.

Breecker D O, Bergel S, Nadel M, et al. 2015. Minor stable carbon isotope fractionation between respired carbon dioxide and

bulk soil organic matter during laboratory incubation of topsoil. Biogeochemistry, 123(1): 83–98.

Bremer E, Janzen H H, Johnston A M. 1994. Sensitivity of total, light fraction and mineralizable organic matter to management practices in a Lethbridge soil. Canadian Journal of Soil Science, 74(2): 131–138.

Brunn M, Spielvogel S, Sauer T, et al. 2014. Temperature and precipitation effects on $\delta^{13}C$ depth profiles in SOM under temperate beech forests. Geoderma, 235–236: 146–153.

Calabrese S, Mohanty B P, Malik A A. 2022. Soil microorganisms regulate extracellular enzyme production to maximize their growth rate. Biogeochemistry, 158(3): 303–312.

Carvalhais N, Forkel M, Khomik M, et al. 2014. Global covariation of carbon turnover times with climate in terrestrial ecosystems. Nature, 514(7521): 213–217.

Chan K Y, Bowman A, Oates A. 2001. Oxidizible organic carbon fractions and soil quality changes in an Oxic Paleustalf under different pasture leys. Soil Science, 166(1): 61–67.

Chen J, Luo Y Q, van Groenigen K J, et al. 2018. A keystone microbial enzyme for nitrogen control of soil carbon storage. Science Advances, 4(8): eaaq1689, doi: 10.1126/sciadv.aaq1689.

Chen X, Gong L, Li Y M, et al. 2018. Spatial variation of soil organic carbon and stable isotopes in different soil types of a typical oasis. Environmental Science, 39(10): 4735–4743.

Cotrufo M F, Soong J L, Horton A J, et al. 2015. Formation of soil organic matter via biochemical and physical pathways of litter mass loss. Nature Geoscience, 8(10): 776–779.

de Rouw A, Soulileuth B, Huon S. 2015. Stable carbon isotope ratios in soil and vegetation shift with cultivation practices (Northern Laos). Agriculture, Ecosystems & Environment, 200: 161–168.

DeGryze S, Six J, Paustian K, et al. 2004. Soil organic carbon pool changes following land-use conversions. Global Change Biology, 10(7): 1120–1132.

Finzi A C, Abramoff R Z, Spiller K S, et al. 2015. Rhizosphere processes are quantitatively important components of terrestrial carbon and nutrient cycles. Global Change Biology, 21(5): 2082–2094.

Gao J, Li R, Li J J, et al. 2016. Grain size distribution, element migration, and stable carbon isotope characteristics of dolomite weathering profiles in Xinpu, North of Guizhou Province. Acta Ecologica Sinica, 36(5): 1409–1420. (in Chinese)

Gong L, Ran Q Y, He G X, et al. 2015. A soil quality assessment under different land use types in Keriya river basin, southern Xinjiang, China. Soil and Tillage Research, 146: 223–229.

Guan J Q, Song C X, Wu Y D, et al. 2022. Responses of soil active organic carbon fractions and enzyme activities to freeze-thaw cycles in wetlands. Wetlands, 42(5): 36, doi: 10.1007/s13157-022-01553-7.

Gui D, Wu Y, Zeng F, et al. 2011. Study on the oasification process and its effects on soil particle distribution in the south rim of the Tarim Basin, China in recent 30 years. Procedia Environmental Sciences, 3: 69–74.

He L Y, Lu S X, Wang C G, et al. 2021. Changes in soil organic carbon fractions and enzyme activities in response to tillage practices in the Loess Plateau of China. Soil and Tillage Research, 209: 104940, doi: 10.1016/j.still.2021.104940.

Huang F, Ochoa C G, Chen X, et al. 2021. Modeling oasis dynamics driven by ecological water diversion and implications for oasis restoration in arid endorheic basins. Journal of Hydrology, 593: 125774, doi: 10.1016/j.jhydrol.2020.125774.

Huntington T G, Johnson C E, Johnson A H, et al. 1989. Carbon, organic matter, and bulk density relationships in a forested spodosol. Soil Science, 148(5): 380–386.

Jobbágy E G, Jackson R B. 2000. The vertical distribution of soil organic carbon and its relation to climate and vegetation. Ecological Applications, 10(2): 423–436.

Joly F-X, Coq S, Coulis M, et al. 2020. Detritivore conversion of litter into faeces accelerates organic matter turnover. Communications Biology, 3: 660, doi: 10.1038/s42003-020-01392-4.

Kan Z R, Liu W X, Liu W S, et al. 2022. Mechanisms of soil organic carbon stability and its response to no-till: A global synthesis and perspective. Global Change Biology, 28(3): 693–710.

Lal R. 2004. Soil carbon sequestration impacts on global climate change and food security. Science, 304(5677): 1623–1627.

Li J Y, Yuan X L, Ge L, et al. 2020. Rhizosphere effects promote soil aggregate stability and associated organic carbon sequestration in rocky areas of desertification. Agriculture, Ecosystems & Environment, 304: 107126, doi: 10.1016/j.agee.2020.107126.

Li L D, Schaeffer S M. 2020. Stabilization mechanisms of isotope-labeled carbon substrates in soil under moisture pulses and conservation agricultural management. Geoderma, 380: 114677, doi: 10.1016/j.geoderma.2020.114677.

Li T N, Zhang G C, Wang S, et al. 2022. The isotopic composition of organic carbon, nitrogen and provenance of organic matter in surface sediment from the Jiangsu tidal flat, southwestern Yellow Sea. Marine Pollution Bulletin, 182: 114010, doi: 10.1016/j.marpolbul.2022.114010.

Ling H B, Guo B, Xu H L, et al. 2014. Configuration of water resources for a typical river basin in an arid region of China

based on the ecological water requirements (EWRs) of desert riparian vegetation. Global and Planetary Change, 122: 292–304.

Liu L Z, Chen L, Pang D B, et al. 2021. Soil organic carbon distribution patterns and influencing factors in Ningxia typical stand based on stable carbon isotope analysis. Acta Botanica Boreali-Occidentalia Sinica, 41(5): 846–853. (in Chinese)

Liu X, Li F M, Liu D Q, et al. 2010. Soil organic carbon, carbon fractions and nutrients as affected by land use in semi-arid region of Loess Plateau of China. Pedosphere, 20(2): 146–152.

Lu J Y, Yang J F, Keitel C, et al. 2020. Rhizosphere priming effects of *Lolium perenne* and *Trifolium repens* depend on phosphorus fertilization and biological nitrogen fixation. Soil Biology and Biochemistry, 150: 108005, doi: 10.1016/j.soilbio.2020.108005.

Ma L X, Ju Z Q, Fang Y Y, et al. 2022. Soil warming and nitrogen addition facilitates lignin and microbial residues accrual in temperate agroecosystems. Soil Biology and Biochemistry, 170: 108693, doi: 10.1016/j.soilbio.2022.108693.

Malik A A, Puissant J, Buckeridge K M, et al. 2018. Land use driven change in soil pH affects microbial carbon cycling processes. Nature Communications, 9: 3591, doi: 10.1038/s41467-018-05980-1.

Nakamoto T, Komatsuzaki M, Hirata T, et al. 2012. Effects of tillage and winter cover cropping on microbial substrate-induced respiration and soil aggregation in two Japanese fields. Soil Science and Plant Nutrition, 58(1): 70–82.

Nath P C, Sileshi G W, Ray P, et al. 2022. Variations in soil properties and stoichiometric ratios with stand age under agarwood monoculture and polyculture on smallholder farms. CATENA, 213: 106147, doi: 10.1016/j.catena.2022.106174.

Nissenbaum A, Schallinger K M. 1974. The distribution of the stable carbon isotope ($^{13}C/^{12}C$) in fractions of soil organic matter. Geoderma, 11(2): 137–145.

Nottingham A T, Turner B L, Stott A W, et al. 2015. Nitrogen and phosphorus constrain labile and stable carbon turnover in lowland tropical forest soils. Soil Biology and Biochemistry, 80: 26–33.

O'Leary H M. 1981. Carbon isotope fractionation in plants. Phytochemistry, 20(4): 553–567.

Okolo C C, Gebresamuel G, Zenebe A, et al. 2020. Accumulation of organic carbon in various soil aggregate sizes under different land use systems in a semi-arid environment. Agriculture, Ecosystems & Environment, 297: 106924, doi: 10.1016/j.agee.2020.106924.

Peng J, Biswas A, Jiang Q S, et al. 2019. Estimating soil salinity from remote sensing and terrain data in southern Xinjiang Province, China. Geoderma, 337: 1309–1319.

Post W M, Kwon K C. 2000. Soil carbon sequestration and land-use change: processes and potential. Global Change Biology, 6(3): 317–327.

Prommer J, Walker T W N, Wanek W, et al. 2019. Increased microbial growth, biomass, and turnover drive soil organic carbon accumulation at higher plant diversity. Global Change Biology, 26: 669–681.

Rakkar M K, Blanco-Canqui H. 2018. Grazing of crop residues: Impacts on soils and crop production. Agriculture, Ecosystems & Environment, 258: 71–90.

Rovira P, Vallejo V R. 2002. Labile and recalcitrant pools of carbon and nitrogen in organic matter decomposing at different depths in soil: an acid hydrolysis approach. Geoderma, 107(1–2): 109–141.

Rovira P, Romanyà J, Duguy B. 2012. Long-term effects of wildfires on the biochemical quality of soil organic matter: A study on Mediterranean shrublands. Geoderma, 179–180: 9–19.

Schaub M, Alewell C. 2009. Stable carbon isotopes as an indicator for soil degradation in an alpine environment (Urseren Valley, Switzerland). Rapid Communications in Mass Spectrometry, 23(10): 1499–1507.

Sharafatmandrad M. 2019. Soil carbon in arid and semiarid rangelands: Controlling factors. Arabian Journal of Geosciences, 12(9): 310, doi: 10.1007/s12517-019-4489-7.

Sokol N W, Slessarev E, Marschmann G L, et al. 2022. Life and death in the soil microbiome: How ecological processes influence biogeochemistry. Nature Reviews Microbiology, 20(7): 415–430.

Tan W B, Wang G A, Huang C H, et al. 2017. Physico-chemical protection, rather than biochemical composition, governs the responses of soil organic carbon decomposition to nitrogen addition in a temperate agroecosystem. Science of the Total Environment, 598: 282–288.

Trivedi P, Delgado-Baquerizo M, Trivedi C, et al. 2016. Microbial regulation of the soil carbon cycle: Evidence from gene-enzyme relationships. The ISME Journal, 10(11): 2593–2604.

Vázquez C, Iriarte A G, Merlo C, et al. 2016. Land use impact on chemical and spectroscopical characteristics of soil organic matter in an arid ecosystem. Environmental Earth Sciences, 75(10): 883, doi: 10.1007/s12665-016-5655-9.

Walkley A, Black I A. 1934. An examination of the Degtjareff Method for determining soil organic matter, and a proposed modification of the chromic acid titration method. Soil Science, 37(1): 29–38.

Wang C, Wei H W, Liu D W, et al. 2017. Depth profiles of soil carbon isotopes along a semi-arid grassland transect in northern

China. Plant and Soil, 417: 43–52.

Wang C, Houlton B Z, Liu D, et al. 2018. Stable isotopic constraints on global soil organic carbon turnover. Biogeosciences, 15(4): 987–995.

Wiesmeier M, Urbanski L, Hobley E, et al. 2019. Soil organic carbon storage as a key function of soils - A review of drivers and indicators at various scales. Geoderma, 333: 149–162.

Woittiez L S, Turhina S R I, Deccy D, et al. 2019. Fertiliser application practices and nutrient deficiencies in smallholder oil palm plantations in Indonesia. Experimental Agriculture, 55(4): 543–559.

Wynn J G, Harden J W, Fries T L. 2006. Stable carbon isotope depth profiles and soil organic carbon dynamics in the lower Mississippi basin. Geoderma, 131: 89–109.

Xiao D, Ye Y Y, Xiao S S, et al. 2019. Tillage frequency affects microbial metabolic activity and short-term changes in CO_2 fluxes within 1 week in karst ecosystems. Journal of Soils and Sediments, 19(10): 3453–3462.

Xue J, Gui D W, Lei J Q, et al. 2019. Oasification: An unable evasive process in fighting against desertification for the sustainable development of arid and semiarid regions of China. CATENA, 179: 197–209.

Xue J, Gui D W, Zeng F J, et al. 2022. Assessing landscape fragmentation in a desert-oasis region of Northwest China: patterns, driving forces, and policy implications for future land consolidation. Environmental Monitoring and Assessment, 194(6): 394, doi: 10.1007/s10661-022-10038-3.

Yu P J, Han K X, Li Q, et al. 2017. Soil organic carbon fractions are affected by different land uses in an agro-pastoral transitional zone in Northeastern China. Ecological Indicators, 73: 331–337.

Zhang C M, Li L, Lockington D. 2014. Numerical study of evaporation-induced salt accumulation and precipitation in bare saline soils: Mechanism and feedback. Water Resources Research, 50(10): 8084–8106.

Zhang H, Wu J W, Zheng Q H, et al. 2003. A preliminary study of oasis evolution in the Tarim Basin, Xinjiang, China. Journal of Arid Environments, 55(3): 545–553.

Zhang J, Wang X J, Wang J P. 2014. Impact of land use change on profile distributions of soil organic carbon fractions in the Yanqi basin. CATENA, 115: 79–84.

Zhang W. 2016. Analysis of cotton quality characteristics and influencing factors based on new cotton standard in Alar Reclamation Area. MSc Thesis. Urumqi: Xinjiang Agricultural University. (in Chinese)

Zhang Z X, Gao P, Li T, et al. 2021. Carbon isotopic measurements from coastal zone protected forests in northern China: Soil carbon decomposition assessment and its influencing factors. Journal of Environmental Management, 299: 113649, doi: 10.1016/j.jenvman.2021.113649.

Zhao Y F, Wang X, Ou Y S, et al. 2019. Variations in soil $\delta^{13}C$ with alpine meadow degradation on the eastern Qinghai-Tibet plateau. Geoderma, 338: 178–186.

Zhong Z K, Han X H, Xu Y D, et al. 2019. Effects of land use change on organic carbon dynamics associated with soil aggregate fractions on the Loess Plateau, China. Land Degradation & Development, 30(9): 1070–1082.

Zhou Y, Zhang J W, Xu L, et al. 2022. Long-term fertilizer postponing promotes soil organic carbon sequestration in paddy soils by accelerating lignin degradation and increasing microbial necromass. Soil Biology and Biochemistry, 175: 108839, doi: 10.1016/j.soilbio.2022.108839.

Zhu G F, Qiu D D, Zhang Z X, et al. 2021. Land-use changes lead to a decrease in carbon storage in arid region, China. Ecological Indicators, 127: 107770, doi: 10.1016/j.ecolind.2021.107770.